Check for updates

CrystEngComm

Accepted Manuscript

This article can be cited before page numbers have been issued, to do this please use: E. L. Smith, J. Ridout, J. D. Sellars and M. R. Probert, *CrystEngComm*, 2019, DOI: 10.1039/C9CE00870E.

This is an Accepted Manuscript, which has been through the Royal Society of Chemistry peer review process and has been accepted for publication.

Accepted Manuscripts are published online shortly after acceptance, before technical editing, formatting and proof reading. Using this free service, authors can make their results available to the community, in citable form, before we publish the edited article. We will replace this Accepted Manuscript with the edited and formatted Advance Article as soon as it is available.

You can find more information about Accepted Manuscripts in the author guidelines.

Please note that technical editing may introduce minor changes to the text and/or graphics, which may alter content. The journal's standard Terms & Conditions and the ethical guidelines, outlined in our author and reviewer resource centre, still apply. In no event shall the Royal Society of Chemistry be held responsible for any errors or omissions in this Accepted Manuscript or any consequences arising from the use of any information it contains.

ROYAL SOCIETY OF CHEMISTRY

rsc.li/crystengcomm

A structural exploration of anisole accessed through extreme conditions crystallisation

View Article Online
DOI: 10.1039/C9CE00870E

Ellie Louvain Smith[a], Joe Ridout[a], Jonathan David Sellars[b] and Michael Richard Probert*[a]

Abstract

Single crystal X-ray diffraction has been used to uncover a new polymorph of anisole, C_7H_8O, at elevated pressure. Structural comparisons have been made to the known, low temperature, form which has also been re-investigated. Both polymorphs crystallise in the monoclinic space group $P2_1/c$ with the new high-pressure polymorph exhibiting a much greater packing efficiency than the low-temperature form, enabled by significantly different intermolecular interactions.

Published on 13 June 2019. Downloaded by Newcastle University on 6/13/2019 4:20:08 PM.

CrystEngComm Accepted Manuscript

Introduction

Compounds may exist in solid state forms which are stable over all currently explored, thermodynamically distinct, conditions. There are many examples of this type of compound in the literature, including several liquids that can be crystallised to generate the same polymorph through both high-pressure and low temperature crystallisation (e.g. dichloromethane[1], iodomethane[2] and 1,2-dichlorobenzene[3]). However, there is also a growing number of systems that have been shown to produce distinct polymorphs through these crystallisation methods (e.g. benzene,[4] fluorotoluene,[5] isopropanol[6] and sulfuric acid[7]). Considerations for the formation of unique high-pressure polymorphs have previously included the presence of impurities in the sample chamber, such as fragments of the gasket or the pressure calibrant.[8] One additional mechanism that can be further utilised to induce differences in the solid form obtained is the variation in kinetics of both the high-pressure and low-temperature experiments i.e. the rate of progression across the liquid/solid phase boundary.[9-11]

Anisole (Figure 1) is a simple aromatic ether, that has common uses as a flavouring agent, a precursor to perfumes or as a solvent in chemical reactions. Under ambient conditions anisole exists in the liquid state, therefore non-standard crystallisation techniques must be employed to enable detailed molecular analysis *via* the solid state, by single crystal X-ray diffraction.[12] Such techniques involve the application of pressure or the reduction in temperature to induce crystallisation.[8,13] Previous studies of anisole have been limited to the low temperature regime,[14] with the sample crystallised under cryogenic conditions. Investigation of the high-pressure experimental space for anisole, presented herein, has resulted in the formation of a new polymorph in addition to the previously studied low temperature form. A comparison of the two distinct polymorphs is reported along with complementary density functional theory calculations, to allow accurate comparison of their relative energies in the solid state.

The aim of this study was to observe and explain how the simple organic liquid anisole responds to changes in the external environment used to induce crystallisation and the resultant impact on the molecular packing motif and density of any crystalline forms obtained.

Experimental

Anisole was used as purchased from Sigma-Aldrich, with no additional modification or purification steps prior to crystallisation. The melting point of anisole was determined to be approximately 235 K.

Cryo-crystallisation:
To recreate the results of Seidel and Goddard[8] the low-temperature crystal form was obtained using anisole sealed in a 0.7 mm internal diameter Lindemann capillary. The sample was then mounted on a fixed chi D8 VENTURE X-ray diffractometer equipped with an Oxford Cryosystems N_2 cryostream. The sample was rapidly cooled from room temperature to 180 K at 360 Kh^{-1} to induce crystallisation and yield a microcrystalline powder. The sample was then warmed at 120 Kh^{-1}, and the temperature cycled around the melting point between 233 and 237 K at 60 Kh^{-1}. After several cycles this process yielded a single crystal of suitable quality for

View Article Online
DOI: 10.1039/C9CE00870E

analysis. Upon obtaining this crystal the sample was cooled to well below its melting point and diffraction data were collected at 225 K. The additional cooling was utilised to ensure the stability of the phase throughout the experiment.

High-pressure crystallisation:
The high-pressure environment, used to induce crystallisation, was generated using conventional diamond anvil techniques. The cell (DAC) used was a modified Merrill-Bassett with 0.8 mm culet, type Ia, diamonds seated in tungsten carbide supports. A stainless-steel gasket of 0.25 mm thickness was pre-indented to a thickness of 0.14 mm. The cylindrical sample chamber of 0.3mm diameter was drilled, through the centre of the indented steel, using an electric discharge machine. Crystallisation and crystal growth stages are shown in (Figure 2a-i). Anisole was loaded into the DAC with a ruby sphere and the cell sealed (2a). The pressure was increased under direct observation until a multi-crystalline phase was formed (2b). The pressure was reduced until the initial melting of the micro-crystallites was observed (2c). Finally, pressure cycling about the melting point at ambient temperature ultimately yielded a single crystal (d-f). This crystal was then grown by slowly increasing the pressure until it filled a large volume of the sample chamber. The final pressure was measured, using the Ruby R_1 fluorescence method,[15] to be 5.8(5) kbar and was kept at this pressure for the single crystal data collection.
The high-pressure data were collected using the XIPHOS diffraction facility at Newcastle University,[16,17] using a Ag X-radiation (λ = 0.56086 Å) source to provide the bright, short, wavelength radiation that is ideal for high-pressure data collection.

Computational analysis:
In order to explore the relative energies of the different polymorphs observed, data from the converged crystal structure refinements (high pressure and low temperature) were used to generate initial coordinates for density functional theory calculations. Geometry optimisations were performed using the density functional theory total energy program CASTEP[18,19] using the PBE[20] exchange correlation functionals and on the fly calculated atomic psuedopotentials. Geometry optimisation was chosen over a simple single point energy calculation to remove the inherent error in the positioning of hydrogen atoms in X-ray crystal structure determinations. Both input and output files detailing the calculations are included in the supplementary information where k-point grids, plane-wave cutoffs and convergence criteria can be found.

Results and Discussion

Both structures were solved and refined using the OLEX2[21] interface to the SHELX[22] suite of programs. The low-temperature polymorph was again found to crystallise in the monoclinic space group $P2_1/c$, with two independent molecules in the asymmetric unit i.e. the results was consistent with the published work of Seidel and Goddard.[8] The principal interactions demonstrated in this solid-state form are of weak intermolecular C-H···π and C-H···O of the type shown in Figure 3.

Polymorph	Interaction	Distance/Å
LT	C-H···O	2.722(1)
		2.7313(9)
		2.8471(9)
	C-H···π	2.7925(6)
HP	C-H···O	2.747(4)
		2.786(6)
	C-H···π	2.750(2)

Table 1 Principal interactions in the 2 polymorphs of anisole

Published on 13 June 2019. Downloaded by Newcastle University on 6/13/2019 4:20:08 PM.

CrystEngComm Accepted Manuscript

View Article Online
DOI: 10.1039/C9CE00870E

The high-pressure polymorph also crystallised in the monoclinic space group $P2_1/c$ with significantly different unit cell parameters and only one molecule in the asymmetric unit. The principal interactions in this form follow those expected from the low-temperature polymorph. Both C-H···π and C-H···O interactions can be identified. These interactions display a markedly different motif to the low-temperature structure as highlighted in Figures 4 and 5. The first coordination can be described in the low-temperature structure as a head to tail motif whereas in the high-pressure form it is dominated by head to head interactions.

The principal intermolecular interaction distances for both polymorphs are highlighted in Table 1. Both forms of the structure can be described as bilayers of anisole, with energetically beneficial intra-bilayer interactions. These interactions appear to be driven by weak dispersion energies or simple packing arguments. The network of interactions in the low-temperature polymorph is significantly more complex than that in the high-pressure one, with the relative orientation of the molecules also differing. The greater complexity of the interaction network displayed by the low-temperature form, and the impact on the entropic energy term this would have, suggests that the nucleation and growth of this polymorph would be slower than the simpler high-pressure form. Therefore, the high-pressure form could be assigned to the kinetic product and the low-temperature to the thermodynamic.

Detailed analysis of the low temperature and high-pressure forms allow the differences between the structures to be observed on the local and global scales. The global differences can be clearly observed by analysing the packing of the molecules (Figures 4 - 7).
In the low-temperature polymorph, the anisole molecules can be described as having a double layered herringbone motif when viewed along the [101] direction (Figure 6). The molecules in the high-pressure polymorph can be described in a similar way along the same orientation, however exhibiting a single layer motif (Figure 7). The orientation of the anisole molecules is striking across the two forms with the high-pressure structure showing a reduced alignment in this direction. The molecules in the low temperature form are orientated in such a way that the plane of the phenyl rings is approximately aligned down the [101] direction with little overlap between each “bone” in the herringbone motif. In contrast, the molecules in the high-pressure polymorph are no longer aligned down the [101] direction and are instead skewed out-of-plane, this enables the “bones” to significantly overlap with one another. Hence as would be expected the applied pressure induces more compressed herringbone layers. This is further demonstrated with the high-pressure polymorph possessing a much greater packing efficiency, and subsequently a much higher density than the low-temperature polymorph. This feature is reflected in the percentage of occupied space for the structures, which was found to be 60.7 % in the low-temperature polymorph and 63.9 % in the high-pressure polymorph, using the default options for the CALCVOID function within the OLEX2 package.

At the local molecular level in the low-temperature polymorph, packing of anisole molecules appears to follow an electrostatic orientation with two principal interactions. The first is observed from the oxygen atom to the meta position of a neighbouring anisole whilst the second is from the meta position of anisole to a neighbouring anisole at the oxygen. Both interactions can be accounted for through resonance structures which demonstrate the oxygen and meta position of anisole possess a partial positive charge and a partial negative charge at the ortho position (Figure 4). These interactions indicate that the structure has been formed through optimisation of well understood, weak, induced dipole interactions suggesting that this form has adopted the "thermodynamic" product in terms of packing energies.

In contrast, the high-pressure polymorph comprises an electrostatically poor set of interactions which do not adhere to the expected electrostatically induced dipoles of anisole (Figure 5). A more random orientation, brought about by the rapid onset of pressure, appears to give rise to a "kinetic" product driven by optimisation of space filling. This is fully consistent with the observed densities of the structures.

Finally, the theoretical calculations confirm the relative energies of the 2 polymorphs, with the low temperature form being the most stable, as shown by a lower total energy of 7.75 kJmol^{-1}. This energy difference is considerable when compared to the extensive work of Nyman and

Published on 13 June 2019. Downloaded by Newcastle University on 6/13/2019 4:20:08 PM.

CrystEngComm Accepted Manuscript

View Article Online
DOI: 10.1039/C9CE00870E

Day[23], where differences of >7.2 kJmol^{-1} are only observed in 5% of all polymorphs. This highlights the extreme impact of elevating pressures compared to reducing temperatures of compounds that are liquid under ambient conditions. However, it is surprising that simple electrostatic arguments or induced dipole interactions can be used to correctly place the relative energies of the systems.

	LT polymorph	HP polymorph
Empirical formula	$C_7H_8O_1$	
Formula weight	108.13	
Temperature (K)	225.0 (2)	ambient
Pressure (kbar)	ambient	5.8 (5)
Habit	irregular	cylinder
Size (mm^3)	0.1 x 0.08 x 0.07	0.25 x 0.25 x 0.1
Crystal system	monoclinic	
Space group	$P2_1/c$	
Z, Z'	8, 2	4, 1
a (Å)	13.6132(7)	13.700(4)
b (Å)	14.5917(8)	5.4468(8)
c (Å)	6.2617(3)	7.8567(11)
β (˚)	95.935(2)	98.401(18)
Volume	1237.16	580.0(2)
Dcalc (gcm^{-3})	1.161	1.238
μ (mm^{-1})	0.607	0.052
Reflections collected	17860	2664
Data/restraints/parameters	2126/0/147	326/51/74
Goodness-of-fit on F^2	1.103	1.133
Final R indexes [I>=2σ(I)]	R_1= 0.0511, wR_2= 0.1523	R_1= 0.0362, wR_2= 0.0730
Final R indexes [all data]	R_1= 0.0544, wR_2= 0.1557	R_1= 0.0616, wR_2= 0.0898
Largest diff. peak/hole (e/Å^{-3})	0.17/-0.20	0.09/-0.09

Table 2 summary crystallographic data for both low-temperature and high-pressure polymorphs of anisole

Conclusions

Two polymorphs of anisole, including a previously unobserved form, have been isolated through two thermodynamically distinct crystallisation methods. One polymorph was grown via cryo-crystallisation, the other through high-pressure crystallisation. Both polymorphs have been fully characterised and found to have diverse packing motifs and densities that have been explored in detail and suggest one form, the low-temperature product, to be the most thermodynamically stable. This suggestion has been confirmed through high level computational calculations where an extraordinary difference in energies for the two forms was observed.

Conflicts of interest

There are no conflicts to declare

Acknowledgements

Published on 13 June 2019. Downloaded by Newcastle University on 6/13/2019 4:20:08 PM.

CrystEngComm Accepted Manuscript

View Article Online
DOI: 10.1039/C9CE00870E

The authors are grateful to Bruker UK Ltd, the EPSRC and Newcastle University for financial support. The authors would also like to that Prof. S. Clark of Durham University for CASTEP calculations.

Notes and references

The authors declare no competing financial interest. Full crystallographic information can be accessed through the deposited data CCDC 1875315 and 1875316

‡ Footnotes relating to the main text should appear here. These might include comments relevant to but not central to the matter under discussion, limited experimental and spectral data, and crystallographic data.

§

§§

etc.

1 M. Podsiadlo, K. Dziubek and A. Katrusiak, *Acta Crystallogr., Sect. B: Struct. Sci*., 2005, **61**, 595-600.
2 M. Podsiadlo and A. Katrusiak, *CrystEngComm*, 2009, **11**, 1951-1957.
3 M. Bujak ,K. Dziubek and A. Katrusiak, *Acta Cryst.,* 2007, **B63**, 124-131.
4 R.J. Fourme, D, Andre and M. Renaud, *Acta Crystallogr., Sect. B: Struct. Sci.*, 1971, **27**, 1275-1276.
5 J. Ridout and M. R. Probert, *Cryst. Growth Des*., 2013, **13**, 1943-1948.
6 J. Ridout and M. R. Probert, *CrystEngComm*, 2014, **16**, 7397-7400.
7 D.R. Allan, S.J. Clark, A. Dawson, P.A. McGregor and S. Parsons, *J. Chem. Soc., Dalton Trans.,* 2002, 1867-1871.
8 E.V. Boldyreva, *Acta Crystallogr., Sect. A: Found. Crystallogr*., 2008, **64**, 218-231.
9 A.R. Choudry, K. Islam, M.T. Kirchner, G. Mehta and T.N. Guru Row, *J. Am. Chem. Soc*., 2004, **126**, 12274-12275.
10 A.M. Dikundwar, R. Sathiskumar, T.N. Guru Row and G.R. Desiraju, *Cryst. Growth Des*., 2011, **11**, 3954-3963.
11 J. Ridout, L.S. Price, J.A.K. Howard and M.R. Probert, *Cryst. Growth Des*., 2014, **14**, 3384-3391.
12 J.A.K. Howard and M.R. Probert, *Science*, 2014, **343**, 1098-1102.
13 R. Lee, J.A.K. Howard, M.R. Probert and J.W. Steed, *Chem. Soc. Rev*., 2014, **43**, 4300-4311.
14 R.W. Seidel and R. Goddard, *Acta Cryst.,* 2015*,* **C71**, 664-666.
15 G.J. Piermarini, S. Block, J.D. Barnett and R.J. Forman, *J. Appl. Phys*., 1975, **46**, 2774-2780.
16 M.R. Probert, J.A. Coome, A.E. Goeta and J.A.K. Howard, *Acta Crystallogr., Sect. A: Found. Crystallogr*., 2011, **67**, 528.
17 M.R. Probert, C.M. Robertson, J.A. Coome, J.A.K. Howard, B.C. Mitchell and A.E. Goeta*, J. Appl. Crystallogr*., 2010, **43**, 1415-1418.
18 M.D. Segall, P.J.D. Lindan, M.J. Probert, C.J. Pickard, P.J. Hasnip, S.J. Clark and M.C. Payne, *J. Phys.: Condens. Matter,* **14,** 2002, 2717–2744.
19 S.J. Clark, M.D. Segall, C.J. Pickard, P.J. Hasnip, M.I.J. Probert, K. Refson and M.C. Payne*l, Z. Kristallogr.,* **220**, 2005, 567–570.
20 J.P. Perdew, K. Burke, M. Ernzerhof, *Phys. Rev. Lett.*, 1996, **77**, 3865; J.P. Perdew, K. Burke, M. Ernzerhof, *Phys. Rev. Lett.*, 1997, **78**, 1396 (E).
21 O.V. Dolomanov, L.J. Bourhis, R.J. Gildea, J.A.K. Howard, H. Puschmann, *J. Appl. Crystallogr*., 2009, **42**, 339-341.
22 G.M. Sheldrick, *Acta Cryst*., 2015, **C71**, 3-8.
23 J. Nyman and G.M. Day, *CrystEngComm*, 2015,**17**, 5154-5165**.**

Published on 13 June 2019. Downloaded by Newcastle University on 6/13/2019 4:20:08 PM.

CrystEngComm Accepted Manuscript

View Article Online
DOI: 10.1039/C9CE00870E

Figures:

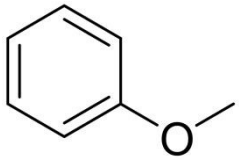

Figure 1 chemical structure of anisole.

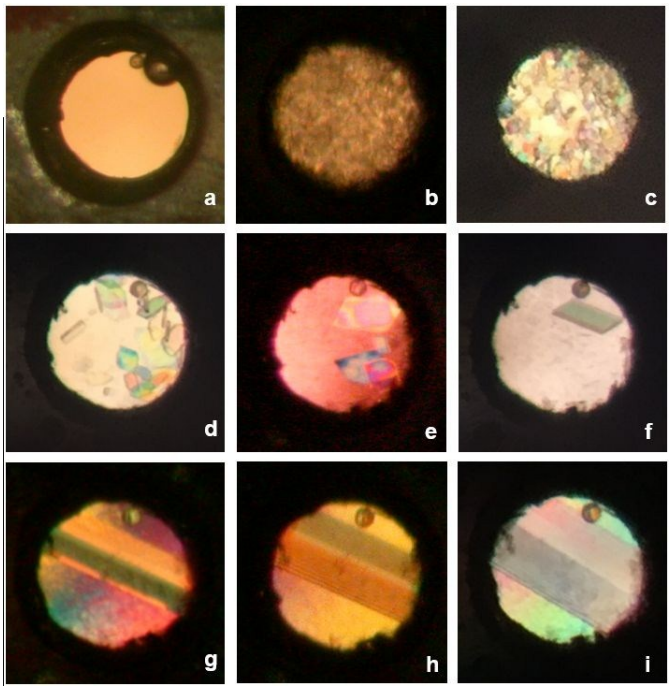

Figure 2 crystallisation and crystal growth at high pressure, pressure increasing from top left (a) to bottom right (i), the hole aperture is 0.25 mm in diameter.

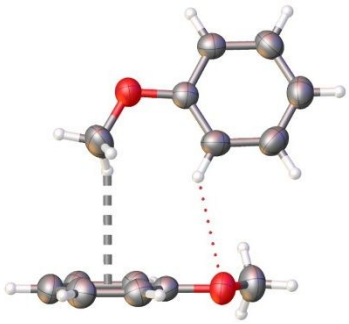

Figure 3 predominant intermolecular interaction types in both forms of anisole comprise C-H···π and C-H···O interactions.

Published on 13 June 2019. Downloaded by Newcastle University on 6/13/2019 4:20:08 PM.

CrystEngComm Accepted Manuscript

View Article Online
DOI: 10.1039/C9CE00870E

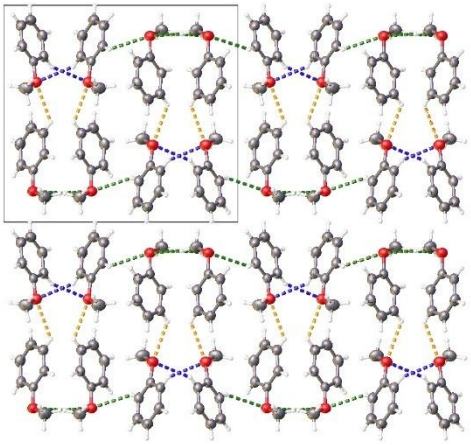

Figure 4 packing diagram of the low-temperature polymorph of anisole with key molecular interactions marked as dashed bonds, viewed down the c-axis. Electrostatic interactions highlighted with blue, green and yellow dashed lines.

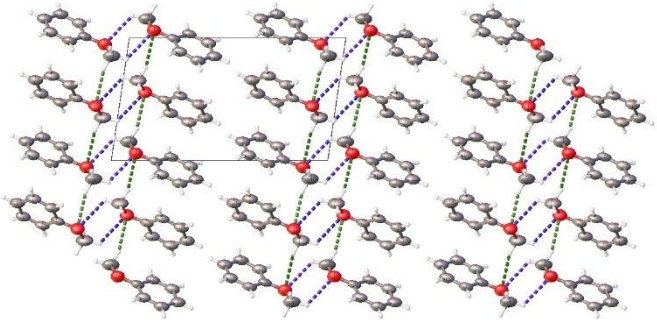

Figure 5 packing diagram of the high-pressure polymorph of anisole with key molecular interactions marked as dashed bonds, viewed down the b axis. Electrostatic interactions highlighted with blue and green dashed lines.

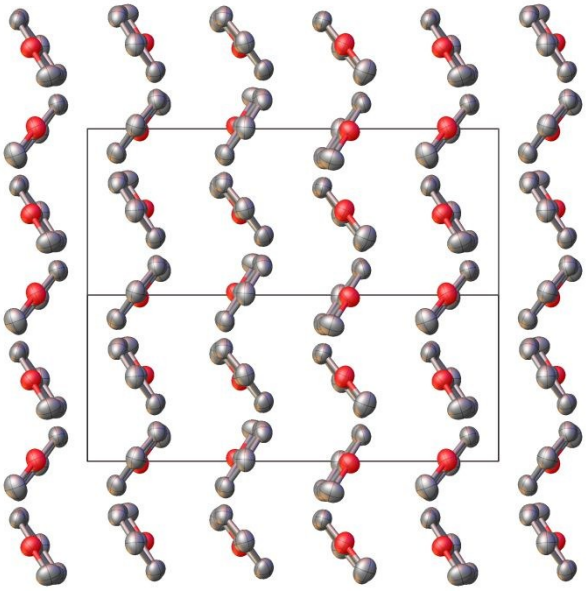

Published on 13 June 2019. Downloaded by Newcastle University on 6/13/2019 4:20:08 PM.

CrystEngComm Accepted Manuscript

View Article Online
DOI: 10.1039/C9CE00870E

Figure 6 packing diagram showing the double herringbone motif of the low temperature polymorph of anisole viewed along the [101] direction.

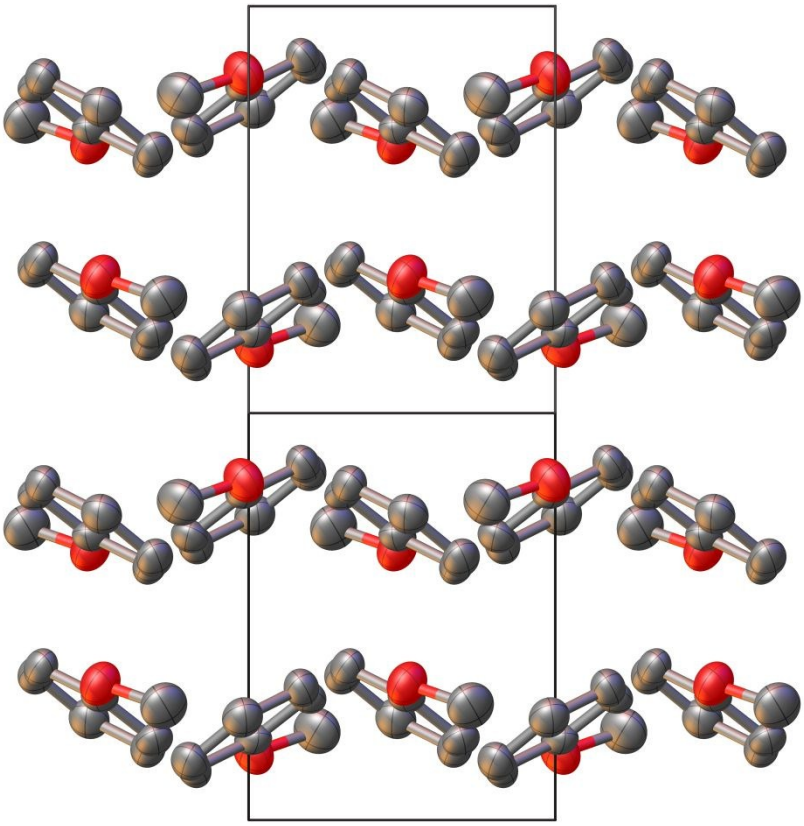

Figure 7 packing diagram showing the single herringbone motif of the high-pressure polymorph of anisole viewed along the [101] direction.

Published on 13 June 2019. Downloaded by Newcastle University on 6/13/2019 4:20:08 PM.

CrystEngComm Accepted Manuscript

View Article Online
DOI: 10.1039/C9CE00870E

Published on 13 June 2019. Downloaded by Newcastle University on 6/13/2019 4:20:08 PM.

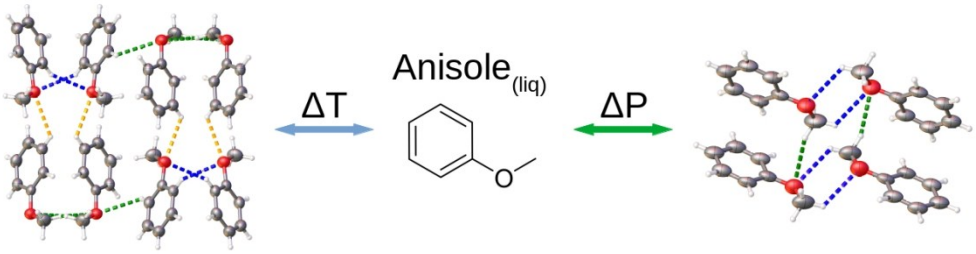

Full size graphical abstract image

111x34mm (300 x 300 DPI)

CrystEngComm Accepted Manuscript

View Article Online
DOI: 10.1039/C9CE00870E

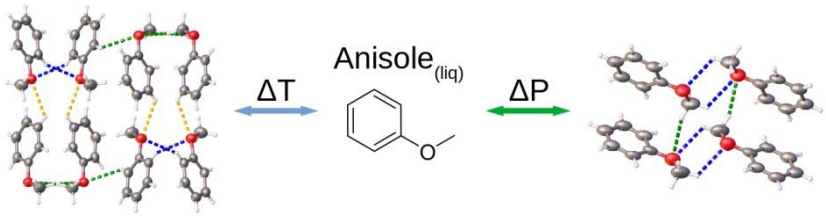

A novel high pressure polymorph of anisole has been discovered and investigated with respect to the known low temperature form

Published on 13 June 2019. Downloaded by Newcastle University on 6/13/2019 4:20:08 PM.

CrystEngComm Accepted Manuscript